Crystalline phase and orientation control of manganese nitride grown on MgO(001) by molecular beam epitaxy

Haiqiang Yang, Hamad Al-Brithen, Eugen Trifan, David C. Ingram, and Arthur R. Smith[a)]
Department of Physics and Astronomy, Ohio University, Athens, Ohio 45701

The phase and orientation of manganese nitride grown on MgO(001) using molecular beam epitaxy are shown to be controllable by the manganese/nitrogen flux ratio as well as the substrate temperature. The most N-rich phase, θ phase (MnN), is obtained at very low Mn/N flux ratio. At increased Mn/N flux ratio, the next most N-rich phase, the η phase (Mn_3N_2), is obtained having its c axis normal to the surface plane. Further increasing the Mn/N flux ratio, the η phase (Mn_3N_2) having its c axis in the surface plane is obtained. Finally, the ε phase (Mn_4N) is obtained at yet higher Mn/N flux ratio. The structural phase variation with Mn/N flux ratio is due to the kinetic control of the surface chemical composition, which determines the energetically most favorable phase. For a given Mn/N flux ratio, the phase is also found to be a function of the substrate temperature, with the less N-rich phase occurring at the higher substrate temperature. The change of phase with temperature is attributed to the change in the chemical composition resulting from the diffusion of N vacancies. Since the magnetic properties of Mn_xN_y depend on the phase, the Mn/N flux ratio provides a way of directly controlling the magnetic properties. A phase diagram for molecular beam epitaxial growth is presented. © *2002 American Institute of Physics.*
[DOI: 10.1063/1.1425435]

I. INTRODUCTION

Transition metal (TM) nitride materials, such as ScN and TiN, have attracted considerable attention both for their structural (high hardness) and electronic (from metallic to semiconducting) properties.[1–7] Certain TM nitrides, including MnN,[8,9] CoN,[10] and FeN,[11] are also promising due to their potential magnetic properties. Moreover, since III–V magnetic semiconductors such as MnGaAs are under intensive investigation,[12] the possibility of forming a magnetic nitride semiconductor, such as MnGaN, which could take advantage of the unique properties of nitrides, is very attractive.[12–15] In addition, it is also of great interest to explore magnetic nitride layers for the possible formation of ferromagnetic/nitride semiconductor multilayers, which might be used for spintronic applications. It is thus important to investigate the epitaxial growth and properties of magnetic nitrides, and in this article we discuss the case of manganese nitride.

Manganese nitride (Mn_xN_y) is known to form different bulk phases, including θ (MnN), η (Mn_3N_2), ζ (Mn_5N_2, Mn_2N, and $Mn_2N_{0.86}$), and ε (Mn_4N).[8,9,16–24] Both structural and magnetic measurements have been reported for most of these bulk phases, and particular attention has been paid to the θ, η, and ε phases. Both η and θ phases are known to have NaCl-type face-centered-tetragonal (fct) structure at room temperature. For η-Mn_3N_2, the measured Mn:N composition ratio matches very well with the ideal Mn:N composition ratio of 3:2. N vacancies in Mn_3N_2 are found to preferentially incorporate into every third layer, resulting in

an ordered vacancy superlattice, according to the model by Jacobs and Kreiner.[8,20] The ideal Mn:N composition ratio for θ-MnN is 1:1, however, most reported composition ratios have been closer to 6:5, leading some authors to refer to the θ phase as Mn_6N_5 or Mn_6N_{5+x}.[16,17,19] However, little or no evidence has been shown that Mn_6N_5 is an ordered phase; rather, the ratio only indicates the presence of N vacancies, which are randomly incorporated into the octahedral lattice sites.[17] Both θ and η phases have been reported to be antiferromagnetic with Néel temperatures of 650 K[9,18,19] and 925 K,[18] respectively. The ε phase has been reported to be ferrimagnetic with a Curie temperature of 738 K.[21–23] The ε phase is also reported to have face-centered cubic (fcc) structure at room temperature with Mn atoms occupying the eight corner sites and six face-center sites and the N atom located at the body center.[22]

While much has been learned from these prior studies on bulk Mn_xN_y, it is important to investigate the possibility of epitaxial layer growth, which is important for device applications. Recently, Yang *et al.* reported the growth of smooth, epitaxial layers of η-Mn_3N_2 with its c axis parallel to the growth plane on MgO(001) substrates using molecular beam epitaxy (MBE).[25] Yet, as discussed above, there are many phases of manganese nitride, and also different orientations of a given phase may occur. With MBE, it should be possible to control both the phase and the crystalline orientation by varying the growth parameters. In this work, we show how to control the phase and orientation of manganese nitride grown on MgO(001) substrates by varying the Mn/N flux ratio J_{Mn}/J_N and also by varying the substrate temperature T_s. In particular, it is shown that the θ-MnN, η-Mn_3N_2, and ε-Mn_4N can each be grown by varying these parameters.

[a)]Author to whom correspondence should be addressed; electronic mail: smitha2@ohio.edu

To achieve these results, many films have been grown by MBE under different growth parameters, each time beginning with a new substrate. The phases are determined through a combination of reflection high energy electron diffraction (RHEED), x-ray diffraction (XRD), and Rutherford backscattering (RBS). Lattice constants are determined from the data, and these are plotted versus the various growth parameters in order to see the detailed dependence on growth parameter. From the data, a diagram of the phase with its orientation is derived, and some schematic models for the observed phases and orientations are presented.

II. EXPERIMENT

The growth experiments are performed in a custom-designed ultrahigh vacuum system consisting of a MBE chamber coupled to a surface analysis chamber. The MBE system includes a solid source effusion cell for Mn and a rf plasma source for N. After being heated up to 1000 °C for 30 min with the nitrogen plasma turned on, the MgO substrate temperature is lowered to the growth temperature, and the growth begins.

For these experiments, the growth temperature is varied from 250 to 600 °C and is measured by means of a thermocouple in contact with a metal heat shield located directly behind the substrate heater. The nitrogen flow rate is set to about 1.1 sccm (growth chamber pressure $= 1.1 \times 10^{-5}$ Torr) with the rf power set at 500 W. This combination of flow rate and plasma power is known to give an effective N flux $J_N \sim 3.6 \times 10^{14}$ cm^{-2} s^{-1}, which was determined from our previous study of ScN growth in the same system.[5,6] Here, we assume the same value of N flux in the case of Mn$_x$N$_y$ based on the similarity of the bonding geometries; for example, ScN and MnN both have octahedral bonding, and thus the growth mechanism is likely to be similar. The Mn flux is controlled in the range from 3.0×10^{13} to 6.0×10^{14} cm^{-2} s^{-1} and is measured by means of a quartz crystal thickness monitor located inside the growth chamber. Also, the final film thickness, which has a range of 700–3300 Å, is measured using a DEKTAK profilometer, and the growth rate, which is in the range of 35–300 nm/h, is then determined from knowledge of the total growth time.

The growth condition is monitored using RHEED with incident electron beam energy of 20 keV, which enables the determination of the surface crystal symmetry and surface lattice parameters. After removal from the ultrahigh vacuum chamber, the samples are investigated using XRD with Cu K_α x rays to determine the crystal structure and lattice parameters along the direction normal to the substrate surface. RBS is applied to determine the bulk Mn/N composition.

III. RESULTS AND DISCUSSION

A. Structure versus Mn/N flux ratio

Figure 1 shows the typical RHEED patterns for the MgO(001) substrate surface just after heating and cooling down to growth temperature (a) and for the manganese nitride surfaces at different Mn/N flux ratios in increasing order of flux ratio (b)–(e). All patterns were acquired at the
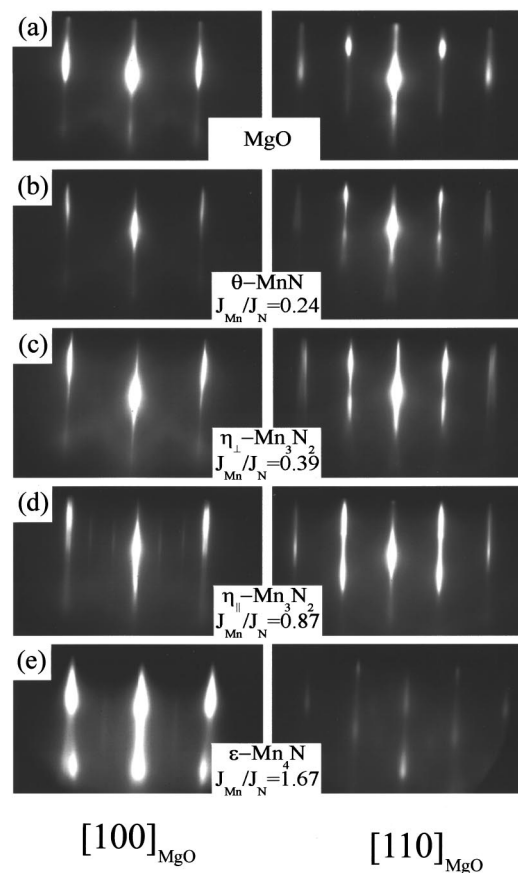
FIG. 1. RHEED patterns of MgO and various phases of manganese nitride grown at a substrate temperature 450 °C: (a) MgO, (b) θ phase (MnN); (c) $\eta_\perp$ phase (Mn$_3$N$_2$), c axis perpendicular to surface; (d) $\eta_\parallel$ phase (Mn$_3$N$_2$), c axis parallel to surface; and (e) ε phase (Mn$_4$N).

growth temperature of 450 °C. Those on the left are with the electron beam along the $[100]_{\text{MgO}}$ direction, while those on the right are with the electron beam along the $[110]_{\text{MgO}}$ direction. All patterns are streaky, indicating that both the starting substrate and film surfaces are smooth.

Since MgO has rocksalt structure with each sublattice having fcc structure, the spacing between first order streaks along $[100]_{\text{MgO}}$ is $4\pi/a_{\text{MgO}}$; along $[110]_{\text{MgO}}$, the RHEED streak spacing is $4\pi/\sqrt{2}a_{\text{MgO}}$. Since the structure of Mn$_x$N$_y$ is similar to that of MgO, the in plane lattice parameters of Mn$_x$N$_y$ corresponding to the spacings between diffraction streaks can be calculated by using $a_{\text{Mn-N}} = a_{\text{MgO}} \times (S_{\text{MgO}}/S_{\text{Mn-N}})$, where $S_{\text{Mn-N}}$ and S_{MgO} are the spacings between first order streaks of manganese nitride and MgO substrate, respectively, and a_{MgO} is the lattice constant of MgO.[26] To obtain the spacing between two diffraction streaks accurately, we fit Lorentzian functions to the streak profiles (obtained by taking a line section of the RHEED data) and then obtain the streak spacing as the difference between the two resulting peak centroids.

Since all the RHEED patterns, including those of the substrate, were obtained at the growth temperature of a given sample, the value for a_{MgO} used to calculate the surface lattice constant for manganese nitride is the value for that temperature, corrected for thermal expansion using the known thermal expansion coefficient for MgO, $\alpha_{\text{MgO}} = 1.3$

$\times 10^{-5}$ K^{-1}.[27] Therefore, the in-plane lattice constants reported here for manganese nitride are for the particular growth temperature. These values will be slightly smaller at room temperature. A separate measurement of the RHEED spacing for η-Mn$_3$N$_2$ showed less than 0.5% change between room temperature and 400 °C; so we expect the measured in-plane lattice parameters to be within 0.5% of the room temperature values.

As seen in Fig. 1(b), for $J_{\mathrm{Mn}}/J_{\mathrm{N}}=0.24$, the RHEED patterns along both directions are very similar to those of MgO. Also, rotations about the sample normal by multiples of 90° show identical RHEED patterns to those in Fig. 1(b). Thus the growth is epitaxial with the substrate and has fourfold symmetric structure. For this flux ratio, the in-plane lattice parameter is determined by the above-described procedure to be 4.22 Å. This value is very close to the reported lattice parameter a of fct θ-MnN, 4.2193 Å.[19] Moreover, it will be shown below that XRD and RBS also confirm the same phase assignment, showing that at the low Mn/N flux ratio, the θ-MnN is obtained.

As shown in Fig. 1(c), for $J_{\mathrm{Mn}}/J_{\mathrm{N}}=0.39$, the RHEED patterns are nearly identical to those of Fig. 1(b) except for a very slight change in the streak spacing, resulting in an in-plane lattice parameter of 4.21 Å. This value is very close to the a of η-Mn$_3$N$_2$, which is reported to equal 4.2046 Å.[19] As discussed below, XRD and RBS confirm that this film has η-Mn$_3$N$_2$ structure with the c axis perpendicular to the surface, which will be referred to as $\eta_{\perp}$.

As shown in Fig. 1(d), for $J_{\mathrm{Mn}}/J_{\mathrm{N}}=0.87$, the RHEED pattern shows additional features not seen at lower flux ratio. In particular, we observe two closely spaced primary diffraction streaks along each $[100]_{\mathrm{MgO}}$ direction. In addition, there are also $\frac{1}{3}$-order fractional streaks along the same directions. The detailed discussion of the structure of this film has been recently reported by Yang *et al.*[25] It is found that the innermost streaks correspond to a ($=4.21$ Å) while the outermost streaks correspond to $c/3$ ($=4.047$ Å) of the fct η-Mn$_3$N$_2$ structure. The $\frac{1}{3}$-order fractional streaks correspond to the superlattice formed by the missing planes of N atoms which occur every third atomic plane in the structural model for the η phase.[8] Thus, for this growth condition, it is found that the c axis of Mn$_3$N$_2$ is parallel to the surface plane; hence, we refer to this phase and orientation as $\eta_{\parallel}$.

As shown in Fig. 1(e), for $J_{\mathrm{Mn}}/J_{\mathrm{N}}=1.67$, the RHEED patterns are not quite as streaky, and some weak additional spots are observed along $[110]_{\mathrm{MgO}}$, suggesting that the film is not as smooth and well ordered as films grown at lower flux ratio. However, fourfold symmetry is still observed, indicating epitaxial growth with the substrate. In addition, weak $\frac{1}{2}$-order fractional streaks are observed along $[100]_{\mathrm{MgO}}$, indicating a 2× periodicity perpendicular to this direction. These observations are all consistent with the ε-Mn$_4$N, which is reported to be fcc with a N atom at the body center.[22] For example, the distance between body centers equals 2× the interatomic row spacing, which explains the $\frac{1}{2}$-order fractional streaks. From the streak spacing, the resulting in-plane lattice parameter is calculated to equal 3.97 Å. This is close to the lattice constant reported for ε-Mn$_4$N (3.87 Å).[22] Although the agreement is not perfect, it will be
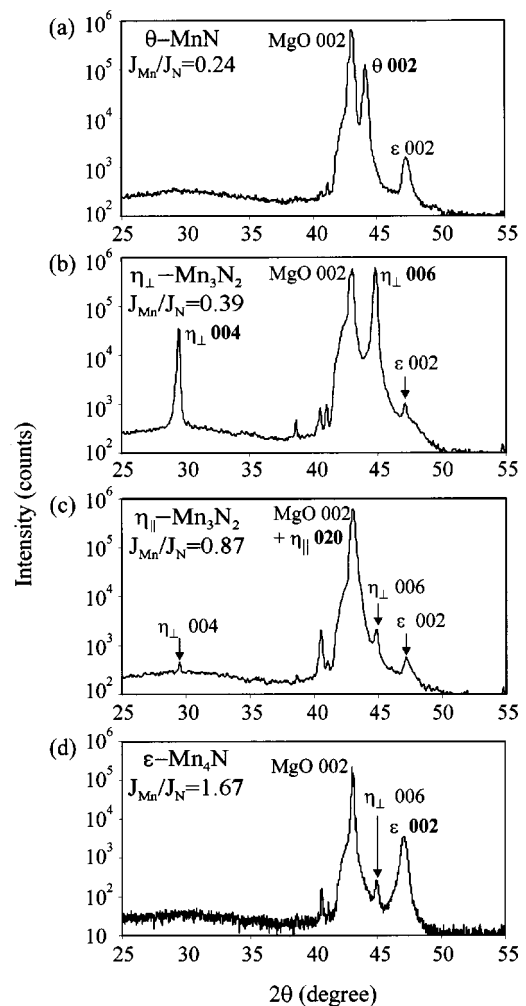
FIG. 2. XRD spectra of various phases of manganese nitride grown at a substrate temperature of 450 °C: (a)–(d) correspond to the RHEED patterns shown in Figs. 1(b)–1(e). The spectra are plotted in semilog scale.

shown below that the XRD and RBS data support the assignment of ε-Mn$_4$N phase.

Figure 2 shows XRD spectra for different manganese nitride films grown on top of MgO(001) in order of increasing Mn/N flux ratio, corresponding to the RHEED patterns presented in Fig. 1. The spectra were obtained at room temperature and are plotted in semilog scale to amplify small peaks. While our x rays include both $K\alpha 1$ and $K\alpha 2$, an average $K\alpha$ wavelength of $\lambda = 1.542$ Å is used to calculate the d spacings. For the substrate, we observe a single diffraction peak at 42.94° giving a d spacing of 2.106 Å. This peak is therefore 002 of MgO corresponding to a lattice constant of 4.213 Å.[26]

As shown in Fig. 2(a), for $J_{\mathrm{Mn}}/J_{\mathrm{N}}=0.24$, XRD shows two major peaks. The first peak at 42.94° is 002 of MgO; the second peak at 43.99° gives a perpendicular d spacing of 2.06 Å. Since $2d$ equals 4.12 Å, which agrees well with the reported value of c for θ-MnN (4.1287 Å),[19] we assign this peak to be 002 of MnN. Combining the RHEED and XRD results together, we conclude the layer is fct θ-MnN with the c axis perpendicular to the surface.

For $J_{\mathrm{Mn}}/J_{\mathrm{N}}=0.39$, we observe a different set of peaks in the XRD spectrum, as shown in Fig. 2(b). The first main

TABLE I. Relative peak intensities of XRD spectra shown in Fig. 2. The intensities of MgO 002 are normalized to 100.00. Columns one and two give the Mn/N flux ratios and the corresponding phases and orientations. Row one gives the corresponding peak indices and positions. Bold indicates the main peak(s) for a given phase.

Mn/N flux ratio	Phase	$\eta_\perp$ 004 29.45°	ε 111 40.44°	MgO 002 42.94°	θ 002 43.99°	$\eta_\perp$ 006 44.81°	ε 002 47.06°
0.23	θ	0.00	0.00	100.00	**19.87**	0.00	0.25
0.40	$\eta_\perp$	**5.82**	0.14	100.00	0.00	**102.52**	0.17
0.93	$\eta_\parallel$	0.06	0.25	**100.00**	0.00	0.26	0.07
1.76	ε	0.00	0.07	100.00	0.00	0.12	**1.58**

FIG. 3. The variation of lattice parameters with Mn to N flux ratio and substrate temperature: (a) lattice parameters vs Mn/N flux ratio: triangles, diamonds, squares, and circles stand for θ phase, $\eta_\perp$ phase, $\eta_\parallel$ phase, and ε phase. Filled markers give a values and empty markers show c or $c/3$ values; (b) lattice parameters vs substrate temperature. The markers have the same meaning as those in (a).

peak is again 002 of MgO at 42.94°; the second main peak occurs at 44.81°, giving a perpendicular d spacing of 2.02 Å. Since 6×2.02 Å equals 12.12 Å, which agrees well with the c of η-Mn_3N_2 which is reported to be 12.131 Å,[19] we conclude that this peak is 006 of η-Mn_3N_2. The third main peak occurs at 29.45°, giving a d spacing of 3.03 Å. Since 4×3.03 Å equals 12.12 Å, which also agrees with c of η-Mn_3N_2, this peak is thus 004 of Mn_3N_2. Combining the RHEED and XRD results, we find that this film has $\eta_\perp$ structure with a = 4.21 Å and c = 12.12 Å with the c axis normal to the growth plane.

For the sample grown at J_{Mn}/J_N = 0.87, only one main peak is observed at 42.94°, as shown in Fig. 2(c). As this peak coincides with that of MgO 002, we conclude that the perpendicular lattice constant is close to that of MgO. As described above based on the RHEED analysis as well as our previously reported result which also made use of scanning tunneling microscopy and neutron scattering (NS) data, this film has the $\eta_\parallel$ structure with the c axis in the plane of the surface. Hence, this XRD result is in good agreement since the perpendicular lattice spacing of this film should be a of Mn_3N_2, 4.21 Å, which is close to a of MgO (4.213 Å).[8,25]

As seen in Fig. 2(d), for J_{Mn}/J_N = 1.67, XRD shows two main peaks, one at 42.94° corresponding to 002 of MgO, the other one at 47.06°, yielding a perpendicular d spacing of 1.93 Å. Since 2×1.93 Å equals 3.86 Å, which agrees very well with the reported a of ε-Mn_4N,[22,28] we assign this peak to be 002 of Mn_4N. Additionally, a small peak at 22.97° is observed (not shown), which gives a d spacing of 3.87 Å. Therefore, this is the 001 peak of Mn_4N. We conclude from RHEED and XRD data that for the Mn/N flux ratio of 1.67, the film has ε-Mn_4N structure.

In addition to the main peaks seen in Figs. 2(a)–2(d), some tiny peaks, such as that at 47.06° corresponding to the 002 peak of ε-Mn_4N, also appear in Figs. 2(a)–2(c). However, the intensities of those peaks are much smaller than the intensities of the main peaks, meaning that for a given flux ratio, the film is mainly single phase with, however, a tiny fraction of other phases present. Another example of this is seen in Fig. 2(c) for the $\eta_\parallel$ phase/orientation in which a tiny fraction of $\eta_\perp$ is also present, as seen by the tiny peaks near 44.81° and 29.45°.

To estimate the phase purity of the various films, Table I shows the normalized intensities of the various XRD peaks for each film, where the intensity of the MgO 002 peak is

normalized to 100.00. The intensities of the primary peaks for each phase are indicated in bold. For the θ phase, the sample was only 1400 Å thick, which explains why the θ 002 peak height is only 20% of the MgO 002 peak height; however, no other major peaks besides the substrate peak are seen. For the $\eta_\perp$ sample (thickness 4700 Å), the 006 peak height is even larger than that of MgO 002. For the $\eta_\parallel$ sample (thickness 3300 Å), the Mn_3N_2 020 peak height cannot be determined because of the overlap with MgO 002; however, the other peaks are extremely small. Finally, for the ε sample (thickness 3300 Å), the height of the 002 peak is less than 2% of the MgO 002 peak. Yet RHEED shows no sign of the $\eta_\parallel$ phase, and no other major peaks are observed. The small ε 002 peak may imply some disorder, misorientation, and/or off-stoichiometry for this growth condition. Yet in all, the results suggest that each sample corresponds to a specific phase of manganese nitride.

Figure 3(a) is a plot of the numerical results for growth at substrate temperature 450 °C, showing the lattice parameters for the four different observed manganese nitride phase/orientations versus the Mn/N flux ratio. Filled markers represent a, and empty markers represent c or $c/3$. In addition to results for the four samples described in Figs. 1 and 2, results for three additional films grown at the same substrate temperature are also shown. As can be seen, the lattice parameters within a given phase are observed to vary slightly with the flux ratio. For example, a and c for the θ phase are both observed to decrease as the Mn/N flux ratio gets smaller. For no set of growth parameters have we observed values of a

and c for the θ phase as large as those reported by Suzuki *et al.*,[9] whereas our $a=4.22$ Å and $c=4.12$ Å for Mn/N flux ratio of 0.24 agree very well with values reported by several other authors, including Lihl *et al.* and Leineweber *et al.*[16,19]

Within the range of Mn/N flux ratio from 0.24 to 0.28,[29] both a and c change abruptly as the phase changes from θ-MnN to $\eta_\perp$. With increasing flux ratio up to 0.39, a increases gradually while $c/3$ remains nearly constant. Within the Mn/N flux ratio range between 0.39 and 0.87,[29] the orientation of the η phase changes from $\eta_\perp$ to $\eta_\parallel$. Finally, within the Mn/N flux ratio range between 0.87 and 1.67, both a and c drop and the phase becomes the ε phase. For growth on MgO(001) at 450 °C, the ζ phase has not been observed, perhaps due to the fact that the ζ phase is reportedly hexagonal, whereas all the other phases have cubic-like structures (fcc or fct) which are likely more compatible with the fcc MgO(001) substrate.

The overall trend is thus as the Mn/N flux ratio increases, the incorporated N fraction decreases, and the next phase occurs which has a higher nominal Mn:N bulk ratio. However, while we have shown that θ, η, and ε phases can each be grown at a single growth temperature, the substrate temperature is still likely to have an important influence on the crystallinity. Indeed, Suzuki *et al.* showed that these phases have different ranges of thermal stability, where the less N-rich phases were stable at higher temperatures. Therefore, it is important to explore the influence of growth temperature on the lattice parameters and phase crystallinity.

Shown in Fig. 3(b) is a plot of the phase and lattice parameters as a function of the substrate temperature. For substrate temperatures between 300 and 450 °C, the a and c of the θ phase each vary by $\sim$1%. Thermal expansion and strain are probably responsible for no more than about 0.5% of the observed variations. The other 0.5% is probably due to variations in Mn/N content. For substrate temperature in the range 500–600 °C, we have not observed the θ phase. This is likely due to the increased diffusion of N atoms, which may lead to N desorption from the surface (probably as N_2) and N vacancy ordering. Here, our results agree well with the annealing study of Suzuki *et al.* who found that the θ phase was not stable above 753 K (480 °C).[9]

The η phase can easily be grown within the same temperature range as for the θ phase but also at temperatures above 450 °C. As seen from Fig. 3(b), with increasing temperature, a increases by $\sim$0.7%, while $c/3$ decreases by $\sim$1%. Thermal expansion and strain effects probably account for $\sim$0.5% of these variations; we attribute at least 0.5% of the variations to a decrease in the incorporated N fraction as substrate temperature increases.

B. Mn/N composition and N vacancies

Shown in Fig. 4 are schematic side-view models for the four phases/orientations of manganese nitride grown on MgO(001) in order of increasing Mn/N flux ratio from (a) to (d). From these models, the strong similarities as well as significant differences between the phases/orientations can be seen. The θ-MnN and η-Mn$_3$N$_2$ are both fct, while the ε-Mn$_4$N is fcc; yet, all three have octahedral bonding. This
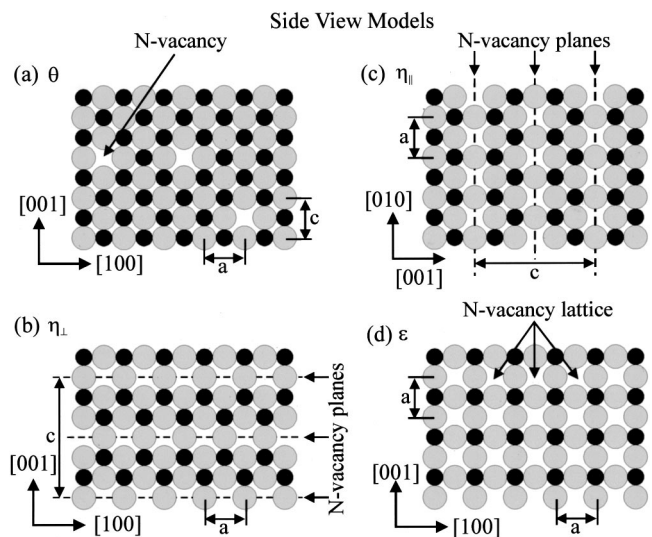
FIG. 4. Side views of schematic model structures of the different phases and orientations. Black dots stand for N atoms; gray circles for Mn: (a) θ phase, (b) $\eta_\perp$ phase, (c) $\eta_\parallel$ phase, and (d) ε phase.

allows one to view all the phases as variations of a simple structure with N vacancies. For example, the θ phase consists of a fct Mn sublattice which is fully occupied together with a fct N sublattice which is also fully occupied but may contain a few N vacancies placed randomly. The other phases can be viewed similarly as consisting of fully occupied Mn fct or fcc sublattices together with N fct or fcc sublattices which have certain fractions of N vacancies.

To see how well the chemical composition of our samples agree with the nominal expected compositions, RBS is performed, and the Mn/N ratio is determined using the RUMP code.[30] Results for the substrate temperature of 300 °C are presented in Table II with the Mn/N ratios shown in row 1. Mn and N are the Mn and N concentrations, respectively, in atoms/unit volume. Row 2 shows the ratio N/(Mn+N), which can be compared with Lihl's reported N contents.[16] Row 3 shows the N fraction defined differently as $f_N = N/2Mn$ (and the Mn fraction $f_{Mn}=Mn/2Mn=50\%$). With this definition, one can define the total N vacancy fraction f_V as equal to $50\% - f_N$. The N vacancy fraction f_V (in %) is shown in row 4 of Table II. Defined this way, the ideal N vacancy fractions for the different phases are: θ-MnN: 0% N vacancies; η-Mn$_3$N$_2$: 16.66% N vacancies; ε-Mn$_4$N: 37.5% N vacancies.

For the θ-MnN phase grown at 300 °C, the RBS results show that N:(Mn+N)=50.0%$\pm$1.0%. This is the only report

TABLE II. Bulk Mn/N composition of the various phases and orientations measured by RBS. The samples are grown at the substrate temperature of 300 °C. The absolute error of each percentage value is 1.0%.

Phase	θ-MnN	$\eta_\perp$-Mn$_3$N$_2$	$\eta_\parallel$-Mn$_3$N$_2$	ε-Mn$_4$N
$\frac{Mn}{N}$	1:1.00	3:2.70	3:2.04	4:1.68
$\frac{N}{Mn+N}$ (%)	50.0	47.0	40.0	30.0
$f_N = \frac{N}{2Mn}$ (%)	50.0	45.0	34.0	21.0
$f_V = 50\% - f_N$ (%)	00.0	5.0	16.0	29.0

so far of ideal 1:1 composition of θ-MnN. Previously reported N contents range from 45.8% to 47.9%.[16] Our sample therefore contains few N vacancies and is consistent with the schematic model of Fig. 4(a).

For the $\eta_\perp$-Mn$_3$N$_2$ phase grown at 300 °C, we find N:(Mn+N)=47.0% ±1.0%. This is quite high in comparison to previously published values for N content ranging from 38.9% to 39.6%; in fact, it falls within the range of previously reported θ phase values.[16] This shows that a N vacancy fraction f_V of only 5% is enough to result in vacancy ordering, as depicted in Fig. 4(b). However, since the N vacancy fraction is so low, the lattice parameters are affected, and we measure $c/3 = 4.08$ Å for this sample, which is in between η (4.04 Å) and θ (4.12 Å).

For the $\eta_\parallel$-Mn$_3$N$_2$ phase grown at 300 °C, we find N:(Mn+N)=40.0% ±1.0%, which agrees exactly with the nominal expected N content for Mn$_3$N$_2$; also, the measured a and c values agree very closely with previously reported values. The measured N vacancy fraction is 16%, and we observe the ordered vacancy structure with the c axis parallel to the surface, as depicted in Fig. 4(c). We attribute the change in orientation from $\eta_\perp \rightarrow \eta_\parallel$ to the increased N vacancy concentration on the surface during growth. For example, the large number of surface N vacancies may be more easily accommodated by forming into parallel vacancy chains, resulting in a surface energy lowering. Indeed, surface vacancy chains have been observed in other systems.[31] The N vacancy chains will then result in the growth of N vacancy planes perpendicular to the surface, and two different rotational domains with their c axes in the surface plane will form, as recently shown by Yang *et al.*[25] There may, however, be an energy cost associated with the formation of the antiferromagnetic domain walls.

Finally, for the ε-Mn$_4$N phase, we find from RBS that N:(Mn+N)=30.0% ±1.0%; this is larger than the expected 20.0%. This shows that a N vacancy fraction $f_V = 29%$ is high enough to result in the ε phase becoming energetically more favorable than the η phase, resulting in the ordering of N vacancies similar to that shown in Fig. 4(d). Note that atomic planes on either side of the one shown would ideally contain no N atoms. For example, the other layers have only Mn atoms arranged in the fcc structure.[22] We also note that the in-plane lattice constant $a_\parallel$ for this sample (3.97 Å) is measured to be 2.5% larger than the perpendicular lattice constant $a_\perp$ (3.87 Å), whereas these two should be equal for ideal fcc structure. Since strain and thermal contraction are not expected to account for more than 1.0% at the most, we suppose the difference is mainly because of two few N vacancies for the ideal 4:1 ratio.

C. Phase diagram for MBE growth

Figure 5 shows the phase diagram of manganese nitride growth by MBE on MgO(001) with substrate temperature shown on the x axis and Mn/N flux ratio shown on the y axis. Different phases are indicated with different symbols, and lines of constant phases are indicated with dashed lines. As can be seen, over a substantial range of growth temperature, we find that the phase depends on the Mn/N flux ratio.
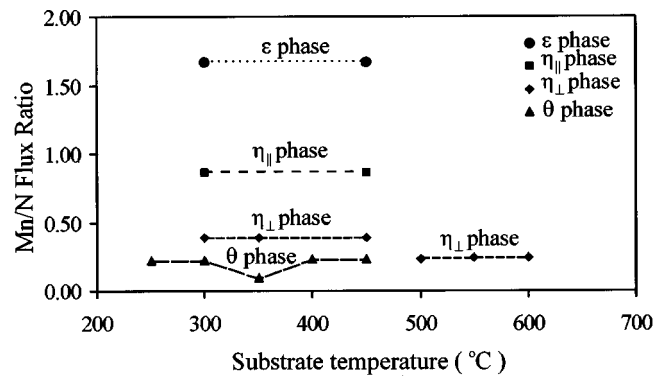
FIG. 5. Phase diagram for MBE growth. Different markers stand for different phases/orientations. The dashed lines indicate lines of constant phase.

Boundaries between phases are not given but lie somewhere between the lines of the constant phase indicated. The θ phase is grown at the lowest Mn/N flux ratios over a wide temperature range from 250 to 450 °C. From 500 to 600 °C, we find $\eta_\perp$ at the same flux ratio. As the flux ratio is increased, we observe the growth of $\eta_\perp$, $\eta_\parallel$, and ε over the substrate temperature range 300–450 °C.

Finally, the magnetic properties of these layers are under investigation. NS studies have already confirmed the layered antiferromagnetic structure of the $\eta_\parallel$ phase.[25] Vibrating sample magnetometry studies have confirmed the ferrimagnetic property of the ϵ phase.[32]

IV. CONCLUSIONS

The growth of manganese nitride on MgO(001) by MBE has been investigated using RHEED, XRD, and RBS. The phase and orientation are shown to be controllable by the MBE growth parameters with the critical growth parameter being the Mn/N flux ratio. In order of increasing flux ratio, the θ, η, and ε phases are each obtained for growth temperatures in the range 300–450 °C. The θ phase is grown with its c axis perpendicular to the sample surface. For the η phase, the orientation of the c axis is perpendicular to the sample surface ($\eta_\perp$) at a lower flux ratio and parallel to the sample surface ($\eta_\parallel$) at a higher flux ratio. At yet a higher flux ratio, the ε phase is obtained.

The detailed lattice parameters have been measured as a function of the flux ratio for various substrate temperatures, and actual Mn:N bulk ratios have been measured for samples grown at 300 °C. Good agreement with many of the previously published lattice parameters for bulk manganese nitride is found, and some variations are discussed in terms of deviations away from ideal stoichiometry. Control of the growth parameters allows the control of the phase and thus the magnetic properties.

ACKNOWLEDGMENTS

J. Appl. Phys., Vol. 91, No. 3, 1 February 2002

Yang *et al.* 1059

[1] J. P. Dismukes, W. M. Yim, and V. S. Ban, J. Cryst. Growth **13/14**, 365 (1972).

[2] T. D. Moustakas, R. J. Molnar, and J. P. Dismukes, Proc.-Electrochem. Soc. **96-11**, 197 (1996).

[3] D. Gall, I. Petrov, P. Desjardins, and J. E. Greene, J. Appl. Phys. **86**, 5524 (1999).

[4] D. Gall, I. Petrov, N. Hellgren, L. Hultman, J. E. Sundgren, and J. E. Greene, J. Appl. Phys. **84**, 6034 (1998).

[5] H. A. H. Al-Brithen and A. R. Smith, Appl. Phys. Lett. **77**, 2485 (2000).

[6] A. R. Smith, H. A. H. Al-Brithen, D. C. Ingram, and D. Gall, J. Appl. Phys. **90**, 1809 (2001).

[7] S. Yang, D. B. Lewis, I. Wadsworth, J. Cawley, J. S. Brooks, and W. D. Munz, Surf. Coat. Technol. **131**, 228. (2000); K. Inumaru, T. Ohara, and S. Yamanaka, Appl. Surf. Sci. **158**, 375 (2000).

[8] G. Kreiner and H. Jacobs, J. Alloys Compd. **183**, 345 (1992).

[9] K. Suzuki, T. Kaneko, H. Yoshida, Y. Obi, H. Fujimori, and H. Morita, J. Alloys Compd. **306**, 66 (2000).

[10] K. Suzuki, H. Morita, T. Kandeko, H. Yoshida, and H. Fujimori, J. Alloys Compd. **201**, 11 (1993).

[11] K. Suzuki, T. Kaneko, H. Yoshida, H. Morita, and H. Fujimori, J. Alloys Compd. **224**, 232 (1995).

[12] H. Ohno, Science **281**, 951 (1998).

[13] T. Dietl, H. Ohno, F. Matsukura, J. Cibert, and D. Ferrand, Science **287**, 1019 (2000).

[14] H. Ohno, Science **281**, 951 (1998).

[15] Y. Ohno, D. K. Young, B. Beschoten, F. Matsukura, H. Ohno, and D. D. Awschalom, Nature (London) **402**, 790 (1999).

[16] F. Lihl, P. Ettmayer, and A. Kutzelnigg, Z. Metallkd. **53**, 715 (1962).

[17] N. Otsuka, Y. Hanawa, and S. Nagakura, Phys. Status Solidi A **43**, K127 (1977).

[18] M. Tabuchi, M. Takahashi, and F. Kanamaru, J. Alloys Compd. **210**, 143 (1994).

[19] A. Leineweber, R. Niewa, H. Jacobs, and W. Kockelmann, J. Mater. Chem. **10**, 2827 (2000).

[20] H. Jacobs and C. Stuve, J. Less-Common Met. **96**, 323 (1984).

[21] G. W. Wiener and J. A. Berger, J. Met. **7**, 360 (1955).

[22] W. J. Takei, R. R. Heikes, and G. Shirane, Phys. Rev. **125**, 1893 (1962).

[23] M. Mekata, J. Phys. Soc. Jpn. **17**, 796 (1962).

[24] M. Mekata, J. Haruna, and H. Takei, J. Phys. Soc. Jpn. **25**, 234 (1968).

[25] H. Q. Yang, H. Al-Brithen, A. R. Smith, J. A. Borchers, R. L. Cappelletti, and M. D. Vaudin, Appl. Phys. Lett. **78**, 3860 (2001).

[26] *Inorganic Index to Powder Diffraction File* (Joint Committee on Powder Diffraction Standards, International Center for Powder Diffraction Data, Swarthmore, PA, 1997) MgO Card No. 04-0820.

[27] H. Landolt and R. Börnstein, *Numerical Data and Functional Relationships in Science and Technology, Group III* (Springer, Berlin, 1975), Vol. 7, Pt. B1, p. 27.

[28] K. M. Ching, W. D. Chang, and T. S. Chin, J. Alloys Compd. **222**, 184 (1995).

[29] Because it is impractical to grow samples at every Mn/N flux ratio, we only give a flux ratio range within which the change occurs.

[30] L. R. Doolittle, Nucl. Instrum. Methods Phys. Res. B **9**, 344 (1985).

[31] F.-K. Men, A. R. Smith, K.-J. Chao, Z. Zhang, and C.-K. Shih, Phys. Rev. B **52**, R8650 (1995).

[32] Professor Y. Ijiri, Oberlin College, Oberlin, OH (unpublished results).